PROCEEDINGS OF SPIE

SPIEDigitalLibrary.org/conference-proceedings-of-spie

Mapping NYF pegmatite outcrops through high-resolution Worldview-3 imagery

D. Santos, A. Mendes, A. Azzalini, J. Cardoso-Fernandes, A. Lima, et al.

D. Santos, A. Mendes, A. Azzalini, J. Cardoso-Fernandes, A. Lima, A. C. Teodoro, "Mapping NYF pegmatite outcrops through high-resolution Worldview-3 imagery," Proc. SPIE 12734, Earth Resources and Environmental Remote Sensing/GIS Applications XIV, 127340U (19 October 2023); doi: 10.1117/12.2675815

SPIE.

Event: SPIE Remote Sensing, 2023, Amsterdam, Netherlands

Mapping NYF pegmatite outcrops through high-resolution Worldview-3 imagery

Santos, D.[1,2]*, Mendes, A.[1], Azzalini, A.[1], J. Cardoso-Fernandes[1,2], Lima, A.[1,2], Teodoro, A.C. [1,2]

[1]Institute of Earth Sciences, FCUP pole, Porto, Portugal; [2] Department of Geosciences, Environment and Spatial Planning Faculty of Sciences of the University of Porto, Portugal;

ABSTRACT

Several studies on remote sensing and mineral exploration have been developed or improved in the last decade. However, the low spatial resolution of satellites is a recurring problem in many cases where the mineral or rock is much smaller than the pixel size of the satellite images. This phenomenon, called sub-pixel occurrence, generates an extremely mixed pixel that difficult the performance of conventional classification algorithms. Satellites with high spatial resolution, such as the Worldview-3 (2 m Ground Sample Distance), have become an essential tool for mineral exploration studies. In addition to its high spatial resolution, the Worldview-3 has 16 bands, 8 in the Visible and Near-infrared (VNIR) and 8 in the Short-Wave Infrared (SWIR) region, which further increases its potential for mineral exploration. This study applies a spectral unmixing-based method, using the Spectral Hourglass Wizard Workflow (SHW), to extract and select pegmatites endmembers from the WorldView-3 images. Further, these endmembers were used for a subpixel classification, performed through Mixture Tuned Matched Filtering (MTMF), to map possible pegmatite outcrops in the Tysfjord pegmatite field, Norway. After classification a high Digital Terrain Model (DTM) hillshade acquired from LiDAR technology and geological data were used to eliminate false positives. The subpixel classification results were compared with geological data and 17 points of interest for pegmatite exploration were selected for further field validation. This work shows the potential of the Worldview-3 high-resolution images processed with a spectral unmixing-based method for mineral exploration in an area of subpixel occurrence. The results are encouraging and show great value for the scientific field of pegmatite exploration.

Keywords: Sub-pixel occurrence; high spatial resolution; mineral exploration; pegmatite; subpixel classification.

*Douglas.santos@fc.up.pt

Earth Resources and Environmental Remote Sensing/GIS Applications XIV, edited by Karsten Schulz, Ulrich Michel, Konstantinos G. Nikolakopoulos, Proc. of SPIE Vol. 12734, 127340U
 · 0277-786X · doi: 10.1117/12.2675815

1. INTRODUCTION

When we talk about remote sensing and mineral exploration, the low Ground Sample Distance (GSD) of the multispectral and hyperspectral satellites is a persistent problem in most cases. The low spatial resolution results in a common problem called subpixel occurrence[1]. In a subpixel occurrence situation, the pixel is much bigger than the target we want to identify. Consequently, the spectrum from that pixels will be mixed, containing information from all the elements present in the pixel[2–4]. In summary, mixed spectra can make the target classification difficult. High-resolution satellite images, such as the WorldView–3 (WV3), can be used to avoid it. The WV3 satellite has 2 m of GSD in Visible and Near Infrared (VNIR) bands, 3.7 m of GSD in Short Wave Infrared (SWIR) bands, and a panchromatic band with 0.5 m of GSD. Besides the better spatial resolution, the WV3 has 16 bands, eight in the VNIR region, and eight bands in the SWIR region. Knowing about the importance of the SWIR region for mineral exploration[5], the spectral resolution of the WV3 plus its high-resolution image put it at an advantage over the open data from satellites such as the LANDSAT 8 / 9, Sentinel 2, and ASTER. However, the potential of WV3 images to identify pegmatites needs to be better investigated. This research tests a spectral unmixing-based method in high-resolution WV3 images aiming to potentialize the identification of new potential Niobium-Yttrium-Fluorine (NYF) pegmatite spots for mineral exploration in Tysfjord, Norway. In this work not only the spectral behavior of open pit mines was analyzed, but also this analysis was used to identify new points of interest for prospecting. Those points of interest were defined through the results obtained regarding the abundance of NYF pegmatites (subpixel classification), identification pixels with pegmatite (Spectral Angle Mapper), and with the support of high-resolution Digital Terrain Model (DTM) Hillshade and geological data to eliminate false positives. The results of this research are intended to compose a fieldwork report identifying anomalies that may be points of interest for NYF pegmatite exploration. This work can be used as a guide to apply the same method in other areas of study.

2. STUDY AREA

The Tysfjord region in northern Nordland, Norway, has a rich geological history, particularly known for the Tysfjord-Hamarøy pegmatite field, which has been a subject of exploration for more than a century[6]. Initially, the region's mining activities focused on ceramic feldspar but later transitioned towards the extraction of high-purity quartz, renowned for its exceptionally low trace element concentrations and extensive use in high-tech products[6]. This intriguing pegmatite field predominantly comprises NYF-type pegmatite bodies and is situated within the geologic context of the Trans-Scandinavian Igneous Belt. The Tysfjord pegmatites have been classified into two distinct genetic groups, namely metapegmatites and pegmatites, based on their age, average size, and degree of deformation, as categorized by Husdal[7]. Müller et al.[8] emphasize that the Tysfjord pegmatites hold a significant abundance of rare elements, believed to have formed through two distinct stages. The first stage dates back to the Svecofennian period, approximately 1.8 billion years ago, and was closely associated with tectonic and metamorphic events. Subsequently, during the Caledonian period, around 430 million years ago, a second stage of formation occurred, involving orogenic and metamorphic processes. The Tysfjord region's pegmatites can be divided into two groups. Group 1 metapegmatites contain diverse minerals, including yttrium-rich fluorite with rare earth elements inclusions, while Group 2 pegmatites are characterized by intense green K-feldspar, black tourmaline, and other minerals. The metapegmatites are unusually large, reaching up to 400 meters, exhibiting an NYF signature, attributed to high fluorine content in the TIB granite gneisses. Group 2 pegmatites have been dated to approximately 400-379 million years old and are believed to have formed as anatetic melts resulting from partial melting of Tysfjord granite gneiss[8]. The study area has two large open pit mines. Hakonhals and Jennyhaugem mines (Figure 1). These mines were chosen as demonstration sites (Ground-truth), so they were of vital importance for this research.

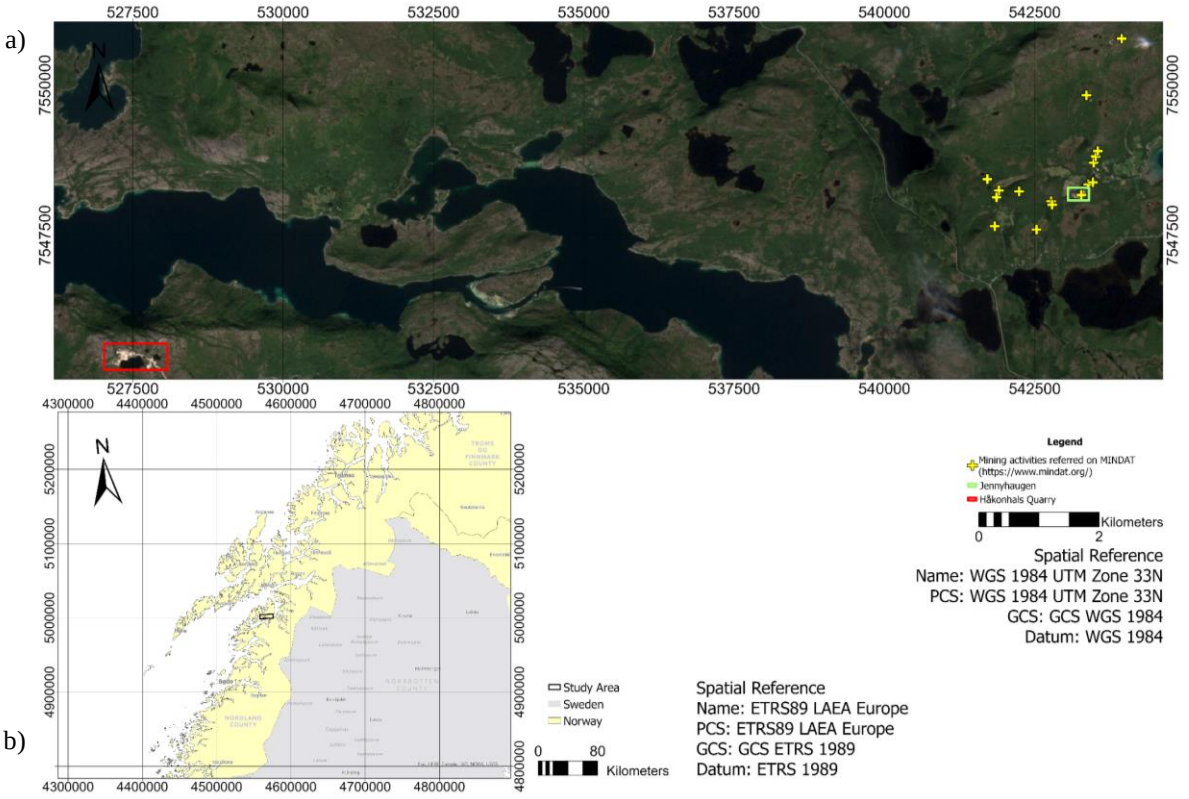

Figure 1. Study area location. The Hakonhals and Jennyhaugen mines are highlighted by the red and green rectangles, respectively. a) An overview of the study area. b) Study area location in Europe.

3. METHODOLOGY

3.1 Data and preprocessing

The WV3 image was acquired on May 23, 2022, on demand. The dataset has eight bands in the VNIR region (with 2 meters of GSD), and eight bands in the SWIR region (with 3.7 meters of GSD). A panchromatic band also is provided with 0.5 meters of GSD. A DTM (Digital Terrain Model) was also acquired, provided by the Norwegian government (Hoydedata.no), and based on LiDAR technology. After the acquisition of the DTM, a hillshade was applied to the terrain topography to help in the interpretation and analysis of the results.

The VNIR, SWIR, and panchromatic bands of WV3 images are provided in separate files. Consequently, before preprocessing the image, it was necessary to perform a layer stacking to combine the SWIR and VNIR bands into a single dataset. To avoid many mosaics, the tiled images were chosen to avoid excessive mosaicking. Orthorectification was applied through the RPC Orthorectification Workflow (ENVI 5.6.3) [9], and the ATCOR Ground Reflectance (PCI Geomatics 2018) was applied to convert the image into surface reflectance. Two tiled images were necessary to cover the study area. One tiled image, in the west of the study area, encompasses the Hakonhals mine (A1), and the other one, in the east, encompasses the Jennyhaugen mine (A2). However, after applying Haze removal to minimize visible haze effects, it was noticed that the Haze removal negatively impacted the tiled image of A2. Thus, it was decided to keep the images separated.

3.2 Spectral Hourglass Wizard (SHW)

To enhance the results of high-resolution WV3 images, spectral unmixing was performed using the SHW workflow. The SHW is a spectral unmixing-based workflow that guides the user through the ENVI hourglass processing flow[10,11]. The Orthorectified tiled image was used as the input in the workflow. The methods applied in the SHW can be divided into three sets: (i) Data dimensionality reduction, (ii) Endmember derivation from the scatter plot, and (iii) Image classification. Data dimensionality reduction was achieved through Minimum Noise Fraction (MNF) and Data dimensionality panel (both performing spectral reduction) and by the Pixel Purity Index (PPI), which selects the most spectrally pure pixels for spatial reduction[12–14]. The n-D Visualizer permits to select and derive the endmembers from a scatter plot while the spectral analyst tool permits to visualize and export the derived endmembers to a spectral library[15–17]. After selecting and deriving the endmembers, they were used for image classification. In this study, two classification methods were applied: Mixture Tuned Matched Filtering (MTMF) and Spectral Angle Mapper (SAM). The step-by-step representation of the Spectral Hourglass Wizard workflow is shown in Figure 2.

3.3 Data dimensionality reduction

The data dimensionality panel indicates several coherent bands and permits modification of the threshold level to separate the signal from the noise[12]. This allows the user to determine spatial coherence more accurately than the MNF. By moving the red line (representing the threshold in Figure 3) above the signal noise[12] the spatial coherence can be determined. In Figure 3, it can be observed that both the threshold (0.78) and the bands above the threshold (4 bands) were the same for A1 and A2. The chosen PPI parameters for A1 and A2 can be observed in Table 1.

Table 1. Parameters used in the Pixel Purity Index calculation.

	Number of iterations	PPI threshold value
A1	15,000	7,500
A2	10,000	5,000

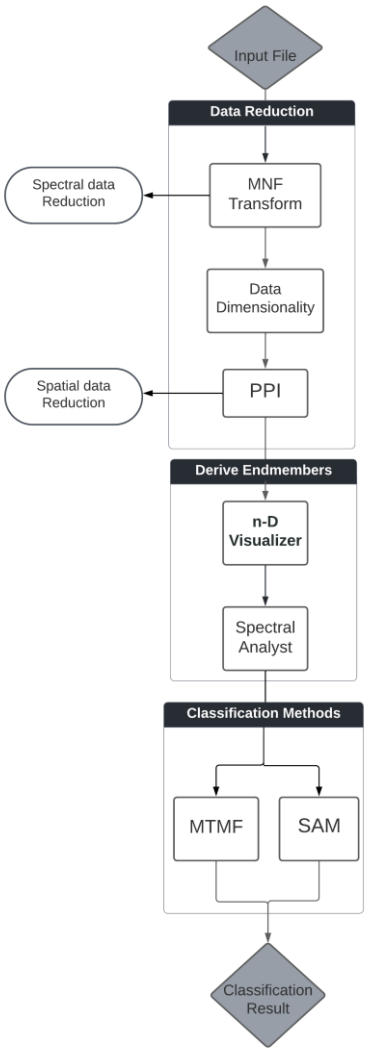

Figure 2. Step by step of Spectral Hourglass Wizard workflow. Adapted from Santos et al.,[18]

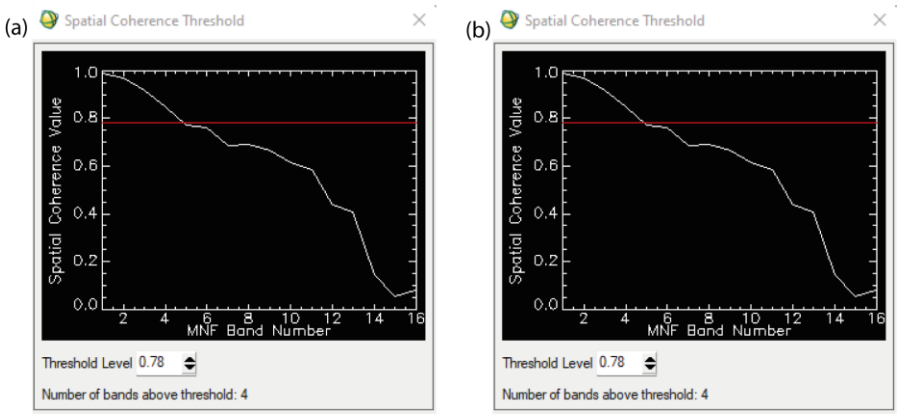

Figure 3. Calculation of data dimensionality. The red line represents the Threshold level. a) Data dimensionality for A1. b) Data dimensionality for A2.

3.4 Derive Endmembers

In this step, it is possible to identify, select, and extract endmembers from the PPI. First, the endmembers from the PPI are plotted in a scatter plot, which can be visualized through the n-dimensional visualizer (n-D Visualiser) tool. Then, it is possible to add more than two dimensions to the scatter plot. Since the endmembers are located at the corners of the data cloud[15,17], we must find the corners and select the endmembers by clusters. After defining the clusters, it is possible to extract the endmembers and visualize them in the spectral analysis tool. The spectral analysis tool allows us to analyze our endmembers by plotting them on a graph[12,18]. While it is possible to compare our endmembers with a known spectral library (such as from USGS[19]), this function, as observed in a previous work[18], did, has not yield acceptable results. Therefore, for this study, the analysis of the endmembers was done by observing the spectral behavior in the SWIR region. Once the spectrum displayed an expected behavior of minerals or hydrothermal alteration rocks in the SWIR region, the image classification was performed. Four endmembers were derived from each image (Figure 4). In Figure 4, it is evident that endmember 3 (A1) and endmember 2 (A2) exhibit a spectral behavior in the SWIR region corresponding to minerals or rocks. Endmember 4 (A1) and 1 (A2) show a spectral behavior corresponding to water. Additionally, the remaining endmembers were identified after classification. That information is summarised in Table 2.

Table 2. Correspondent elements for each endmember extracted from the data cloud.

Endmembers	A1	A2
1	Vegetation	Water
2	Snow	Pegmatite
3	Pegmatite	Snow
4	Water	Vegetation

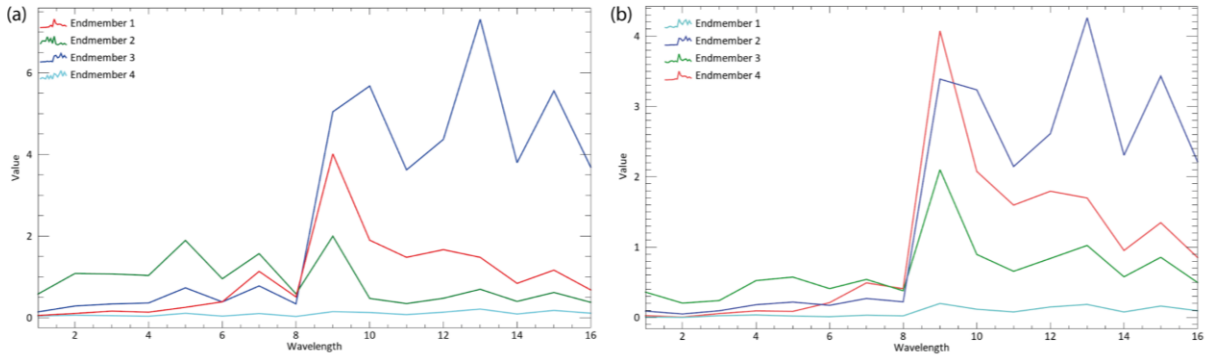

Figure 4. Plot of endmembers derived from data cloud. The pegmatite endmembers are represented in blue colours. a) Endmembers derived from A1. b) Endmembers derived from A2.

3.5 Classification Methods

The MTMF uses Matched Filtering (MF) and infeasibility score to improve the results by, reducing the number of false positives. The MTMF generates a set of rule images corresponding to an MF score for each pixel compared to each endmember. Using the endmembers retrieved through the n-D Visualiser, MTMF resulted in four MF bands that were used for analysis in a GIS environment (QGIS)[1,16,20–22].

The SAM algorithm is defined as a physically-based spectral classification that compares the angle between the endmember spectrum vector and each pixel in n-D space using an n-D angle to match pixels to the reference spectra. Smaller angles threshold represents closer matches to the reference spectrum, while pixels distant from the maximum angle are not classified. The SAM classification helps to analyze the distribution of the elements under study, forming multiple clusters of probable target pixels[10,21]. The maximum angle applied for the classification was 0.10.

4. RESULTS AND DISCUSSION

4.1 Classification Methods

Firstly, the classification results were analyzed in known pegmatite locations to understand the spectral behavior in the NYF pegmatites in Tysfjord. For Ground-truth, the Hakonhals and Jennyhaugen mines were chosen due to their large exposition in open pit mines. As shown in Figure 5 b and c), the MTMF correctly identified the known pegmatite points of Hakonhals and Jennyhaugen. In red colour are the pixels with very high values (240-255) that correspond to the locations with more abundance of NYF pegmatite. In orange colour are the pixels with high values (208-239). In yellowish colour are represented the pixels with values between 176 and 207, while in greenish colour are the pixels with values between 112 and 175. Lastly, in bluish colour are the pixels that correspond to the locations with less abundance of NYF pegmatite (0-111). In the Hakonhals mine, the abundance of NYF pegmatite was correctly identified in the west of the mine, which matches the location of the pegmatite body. The inner paths of the mine were highlighted with lower values, but this can be occasioned by pegmatite vestigial in this path. At Jennyhaugem mine, the MTMF identifies more abundance pixels of very high values in the northwest of the mine, and some lines in the central zone of the mine. The MTMF method was able to identify the abundance of NYF pegmatites in the demonstration sites. On the other hand, the big concentration of the highest values at mines should be caused due the mine pegmatite exploration, which turns the pegmatite and trace elements of the pegmatite more exposed for satellite images. In a natural occurrence, it is expected less abundance of pixels with very high values and more clusters of pixels with high values or less.

As is possible to observe in Figure 5 (d and e), the SAM algorithm assigns the same value for all the pixels classified as pegmatite. This demonstrates that the SAM is less sensitive to identifying the NYF pegmatites than MTMF. However, the mines were correctly identified indicating that this method can be applied to identify pegmatite outcrops.

4.2 Spots of interest for field validation

Analyzing the spectral response of the target, was possible to look for outcrops with similar spectral behavior and highlighted them. To choose the outcrops both MTMF and SAM results were used considering the intersection of the results. As SAM results present more false positives, the MTMF had more influence on decision-making. After choosing the first set of spots, the false positives were eliminated using a high-resolution true-color composite, high-resolution DTM acquired from LiDAR data, and geological data of the area (www.mindat.org). The DTM with one meter of spatial resolution was used for the interpretation of the terrain topography and to validate old mines or pegmatite quarries in the region. Many false positives have been identified in coastal areas and constructions such as roofs of houses and in some cases even the soil surrounding some houses. Therefore, the high resolution of the WV3 true color composition was essential to analyze the results and eliminate false positives.

Initially, 98 possible points of interest were delineated. After eliminating the false positives in the places where there was a very large clustering of points of interest, it was decided to form a polygon representing an area of interest. In total, four areas and 17 points of interest were selected (Figure 6).

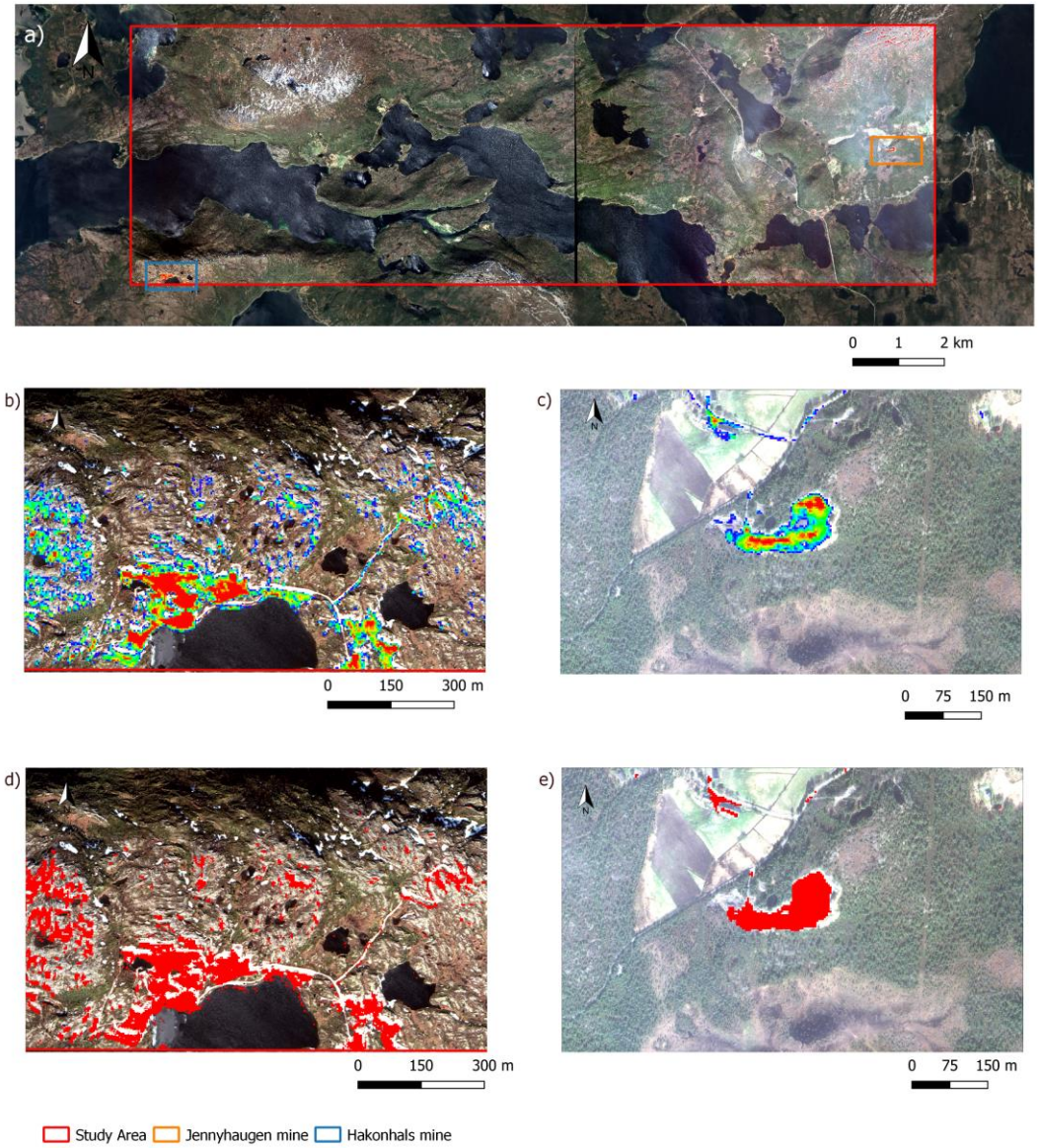

Figure 5. Spectral behavior of the demonstration sites (Hakonhals and Jennyhaugen mines). a) Overview of the study area. b) MTMF results for Hakonhals mine. c) MTMF results for Jennyhaugen mine. d) SAM algorithm results for Hakonhals mine. e) SAM algorithm results for Jennyhaugem mine.

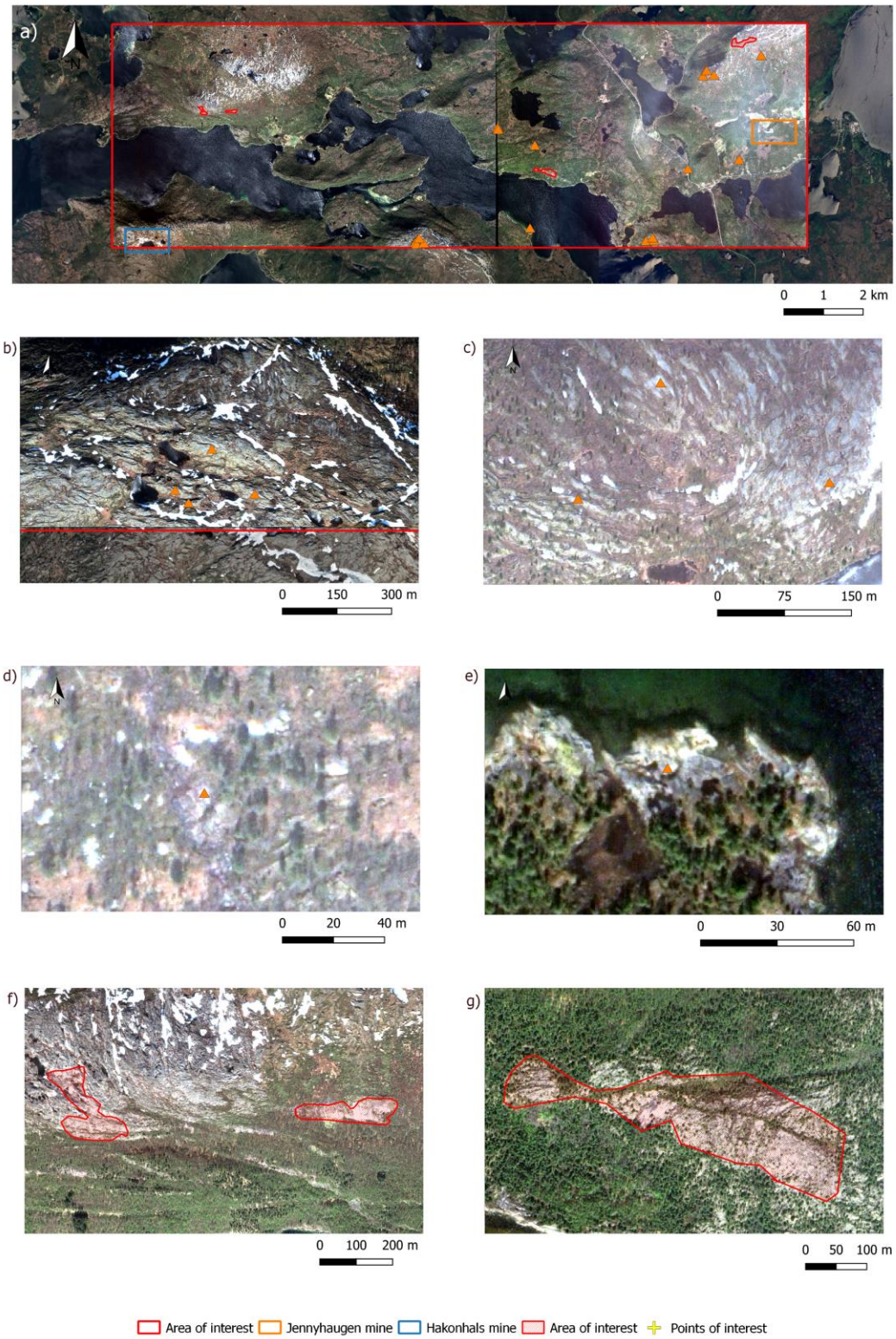

Figure 6. Points and areas of interest for field validation: overview of the study area (a); points of interest represented in yellow crosses (b, c, d, e); areas of interest represented in red polygons (f)-g).

5. CONCLUSIONS

This study applies a spectral unmixing-based approach aiming to enhance the potential of the high-resolution WV3 processing images. At the end of the process, two classification methods were applied: the MTMF and the SAM algorithm. As a subpixel classification method, the MTMF had better results in highlighting the spectral abundance of the NYF pegmatites. Through a color slice composite was possible to see and analyse the distribution of the very high and high pixel values that represent the NYF pegmatite pixels (Figure 5. b and c). The method proposed in this research can be adapted to different areas of study and different targets. However, the presence of two large open pit mines in the study area may have facilitated the obtention of pegmatites NYF endmembers from the data cloud. Even so, spectral unmixing demonstrated to be a powerful tool applied together with high-resolution images. As a result, 17 points and four areas of interest were selected for future fieldwork validation.

ACKNOWLEDGMENTS

This study is funded by European Union's Horizon 2020 innovation program under grant agreement No 869274, project GREENPEG: New Exploration Tools for European Pegmatite Green-Tech Resources. The work was also supported by Portuguese National Funds through the FCT project UIDB/04683/2020 and UIDP/04683/2020 - ICT (Institute of Earth Sciences). Douglas Santos was financially supported by Portuguese national funds through FCT (Grant: UI/BD/154412/2023).

REFERENCES

[1] Hosseinjani Zadeh, M., Tangestani, M. H., Roldan, F. V. and Yusta, I., "Sub-pixel mineral mapping of a porphyry copper belt using EO-1 Hyperion data," Advances in Space Research 53(3), 440–451 (2014).
[2] Quintano, C., Fernández-Manso, A., Shimabukuro, Y. E. and Pereira, G., "Spectral unmixing," International Journal of Remote Sensing 33(17), 5307–5340 (2012).
[3] Zhang, J., Zhang, X. and Jiao, L., "Dual-View Hyperspectral Anomaly Detection via Spatial Consistency and Spectral Unmixing," Remote Sensing 15(13), 3330 (2023).
[4] Clasen, A., Somers, B., Pipkins, K., Tits, L., Segl, K., Brell, M., Kleinschmit, B., Spengler, D., Lausch, A. and Förster, M., "Spectral unmixing of forest crown components at close range, airborne and simulated Sentinel-2 and EnMAP spectral imaging scale," Remote Sensing 7(11), 15361–15387 (2015).
[5] Santos, D., Cardoso-Fernandes, J., Lima, A., Müller, A., Brönner, M. and Teodoro, A. C., "Spectral Analysis to Improve Inputs to Random Forest and Other Boosted Ensemble Tree-Based Algorithms for Detecting NYF Pegmatites in Tysfjord, Norway," Remote Sensing 14(15) (2022).
[6] Mueller, A., Snook, B., Ihlen, P. M., Beurlen, H. and Breiter, K., "Diversity of the quartz chemistry of NYF- and LCT-type pegmatites and its economic implications," Mineral Deposit Research for a High-Tech World, Vols. 1-4(August), 1774–1776 (2013).
[7] Husdal, T., "The minerals of the pegmatites within the Tysfjord granite, northern Norway," Norsk Bergverksmuseum, skrift 38(1906), 5–28 (2008).
[8] Müller, A., Romer, R. L., Augland, L. E., Zhou, H., Rosing-Schow, N., Spratt, J. and Husdal, T., "Two-stage regional rare-element pegmatite formation at Tysfjord, Norway: implications for the timing of late Svecofennian and late Caledonian high-temperature events," International Journal of Earth Sciences 111, 987–1007 (2022).
[9] Pradhan, B., Ahmed, A. A., Chakraborty, S., Alamri, A. and Lee, C.-W., "Orthorectification of WorldView-3 Satellite Image Using Airborne Laser Scanning Data," J Sens 2021 (2021).
[10] Odden, B., Kneubühler, M. and Itten, K. I., "Comparison of a Hyperspectral Classification Method Implemented in Two Remote Sensing Software Packages," Matrix (February) (2005).

[11] Odden, B., Itten, K. I., & Laboratories, R. S., Comparison of a Hyperspectral Classification Method. Matrix, March, 1–8 (2009).
[12] Wolfe, J. D. and Black, S. R., "Hyperspectral Analytics in ENVI" (2018).
[13] Mujabar, P. S. and Dajkumar, S., "Mapping of bauxite mineral deposits in the northern region of Saudi Arabia by using Advanced Spaceborne Thermal Emission and Reflection Radiometer satellite data," Geo-Spatial Information Science 22(1), 35–44 (2019).
[14] Boardman, J. W., Kruse, F. a. and Green, R. O., "Mapping target signatures via partial unmixing of AVIRIS data," Summaries of JPL Airborne Earth Science Workshop, 3–6 (1995).
[15] Gabr, S., Ghulam, A. and Kusky, T., "Detecting areas of high-potential gold mineralization using ASTER data," Ore Geology Reviews 38(1–2), 59–69 (2010).
[16] Rajendran, S. and Nasir, S., "Characterization of ASTER spectral bands for mapping of alteration zones of volcanogenic massive sulphide deposits," Ore Geology Reviews 88, 317–335 (2017).
[17] Hu, B., Xu, Y., Wan, B., Wu, X. and Yi, G., "Hydrothermally altered mineral mapping using synthetic application of Sentinel-2A MSI, ASTER and Hyperion data in the Duolong area, Tibetan Plateau, China," Ore Geol Rev 101(July), 384–397 (2018).
[18] D. Santos, J. Cardoso-Fernandes, A. Lima, and A. C. Teodoro "The potential of spectral unmixing method applied to PRISMA hyperspectral images in the identification of Li minerals: an evaluation for prospecting purposes", Proc. SPIE 12268, Earth Resources and Environmental Remote Sensing/GIS Applications XIII, 1226811 (2022).
[19] Kokaly, R. F., Clark, R. N., Swayze, G. A., Livo, K. E., Hoefen, T. M., Pearson, N. C., Wise, R. A., Benzel, W. M., Lowers, H. A., Driscoll, R. L. and Klein, A. J., "USGS Spectral Library Version 7," Reston, VA (2017).
[20] Salles, R. dos R., de Souza Filho, C. R., Cudahy, T., Vicente, L. E. and Monteiro, L. V. S., "Hyperspectral remote sensing applied to uranium exploration : A case study at the Mary Kathleen metamorphic-hydrothermal U-REE deposit, NW, Queensland, Australia," Journal of Geochemical Exploration 179, 36–50 (2017).
[21] Rajendran, S. and Nasir, S., "Characterization of ASTER spectral bands for mapping of alteration zones of volcanogenic massive sulphide deposits," Ore Geology Reviews 88, 317–335 (2017).
[22] L3Harris., "Mixture Tuned Matched Filtering," <https://www.l3harrisgeospatial.com/docs/mtmf.html> (2 November 2021).